Digest Journal of Nanomaterials and Biostructures Vol. 15, No. 3, July - September 2020, p. 769 - 779

INVESTIGATIONS ON HYDROTHERMAL SYNTHESIS PARAMETERS IN PREPARATION OF ZEOLITE W

X. ZHANG*, Q. LIU, S. YANG
College of Chemistry and Chemical Engineering, Xuchang University, Xuchang, 461000, China

Zeolite W crystals were synthesized via hydrothermal process, the influence of crystallization time, aging time and temperature, the molar ratios Al_2O_3/SiO_2 and K_2O/SiO_2 on the crystalline final products were studied. The results revealed that well-developed twin-ball shaped morphology zeolite W crystals were obtained after 6 h of crystallization, the longer crystallization time would not result in substantial changes in crystal morphology and size of end products. However, the crystals transferred from twin-ball to bouquet-like in shape with increasing aging time, while the high aging temperature resulted in zeolite F developed. Also, the Al_2O_3/SiO_2 and K_2O/SiO_2 molar ratios of the hydrogel had major influences on synthesis of pure form zeolite W. Well-crystallized pure phase zeolite W products were obtained with Al_2O_3/SiO_2=0.20, which were composed of many square pillars crystals, with average width in the range of 0.2–0.5 μm and length approximately 10 μm. Mild alkalinity circumstance was in favor of zeolite W crystallization, when the K_2O/SiO_2 molar ratio was increased to 9.42, the product obtained was pure phase of zeolite LTJ.

(Received March 2, 2020; Accepted August 11, 2020)

Keywords: Zeolite W, Crystallization, Crystal, Morphology, Zeolite LTJ

1. Introduction

Zeolites are crystalline aluminosilicates consisting of SiO_4^{4-} and AlO_4^{5-} tetrahedral [1,2]. The uniformly distributed channels and cavities in zeolites, usually in the size range of about 0.3–1 nm in molecular dimensions, endow them with unique molecular recognition, discrimination and organization properties [3–5]. Among various zeolites, Zeolite W crystal is small-pored zeolite with a channel system made up of three dimensional, interconnected 8-membered ring pores [6]. Zeolite W have been widely used in the field of arsenic adsorption, H_2 storage as well as membrane separation due to its special properties [7,8].

Most of applications of zeolites are mainly depend on their frameworks. However, particulate properties and shapes of zeolite samples also play important roles in the efficiency and mode of their applications. Nowadays, many attempts were aimed at the studies of various factors which controlled the particulate properties and crystallization pathways of zeolite samples [9–11].

* Corresponding author: zxzx5973428@163.com

These results displayed that crystallization, aging and chemical composition of the gel played important roles in controlling the product properties. Valtchev et al [12]. reported that well-developed zeolite NaA crystals were observed after 3 days of crystallization at room temperature, however, further increasing crystallization time, NaA particles continued to grow, as well as the particle size distribution changes. In a more detail study, it can be explained that the nutrients were provided by dissolving the less stable and smaller zeolite nanoparticles. That is, the system entered in the Ostwald ripening stage [13]. Jamil et al [14]. reported the increase of aging time resulted in decrease of crystal length, big ZSM-22 crystals about 13 um in size were obtained after 12 h aging, and the crystal length reached its minimum after 72 h, while the average length was approximately 100 nm. On the other hand, it was also reported that crystal morphology and size remained the same even after 7 d aging, indicating that aging didn't facilitate the nucleation [15]. In addition, Zhang et al [16]. revealed that SiO_2/Al_2O_3 of the gel was very sensitive for zeolite synthesis. When the SiO_2/Al_2O_3 molar ratio varied from 1.5 to 4.0, pure phase zeolite NaX crystals were produced; with SiO_2/Al_2O_3 was 1.0, the co-existence of zeolite NaA with zeolite NaX; only with SiO_2/Al_2O_3 was 0.5, pure phase zeolite NaA was achieved. Moreover, the Si/Al ratio of NaX products obtained increased with increasing SiO_2/Al_2O_3 ratio in the gel. These results of numerous investigations gave very worthy and quality data. However, there were very limited papers reporting on zeolite W synthesis.

Here, we synthesized zeolite W via hydrothermal process. The influences of crystallization time, aging time and temperature, the molar ratios Al_2O_3/SiO_2 and K_2O/SiO_2 on the final products were studied.

2. Experimental details

2.1. Zeolite synthesis

Zeolite W was prepared as followed: sodium aluminate (anhydrous, Merck) and potassium hydroxide (99%, Sigma-Aldrich) were dissolved in deionized water. Afterwards a certain amount of colloidal silica suspension (HS-30, Sigma-Aldrich) was slowly poured into the above solution with strong stirring, and the molar composition of mixture was y K_2O: x Al_2O_3: 1.0 SiO_2: 57 H_2O, where x varied from 0.04 to 0.45 mol and y from 0.15 to 9.42 mol, respectively. The gel was then stirred for 20 min under room temperature, followed by aging for 0–24 h and experienced the hydrothermal crystallization at 150 °C. Finally, the powder product was filtered and thoroughly washed with distilled water, then dried at 90 °C for 24 h.

2.2. Characterization

X-ray diffraction patterns (XRD) were taken by a PhilipsPW 1830 diffractometer with Cu-Kα radiation operated at 20 mA and 40 kV. Transmission IR spectra (FTIR) were made using a Bruker IFS 66 v/S spectrometer with a KBr method. Scanning electron microscopy images (SEM) were obtained on a LEO 1530 TFE microscope.

3. Results and discussions

3.1. Influence of crystallization time

Fig. 1 shows the influence of crystallization time on final products from the gel with mole ratio 1.5 K_2O: 0.1 Al_2O_3: 1.0 SiO_2: 57 H_2O, the gel was then hydrothermally treated at 150 °C without aging. Clearly, the product obtained after 1 h hydrothermal crystallization is totally amorphous (Fig. 1a). Some weak zeolite W peaks are observed after 3 h, implying that a large number of amorphous materials are still existed (Fig. 1b). A fast increase of crystallinity is seen between 3 and 5 h hydrothermal treatment (Fig. 1b–d). A well-developed zeolite W product is obtained after 6 h (Fig. 1e). While the crystallization time is prolonged to 24 h, the relative intensity of diffraction peaks do not further increase, indicating that the crystallization of zeolite W is almost complete within 6 h (Fig. 1f).

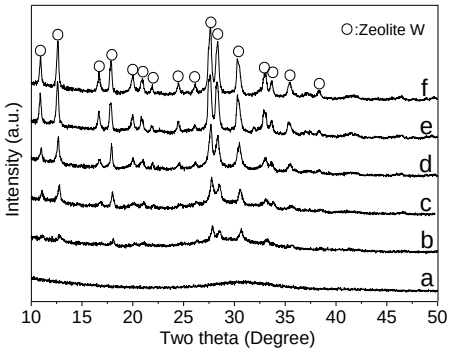

Fig. 1. XRD patterns of products obtained with various crystallization time. (a) 1 h, (b) 3 h, (c) 4 h, (d) 5 h, (e) 6 h and (f) 24 h.

The FT-IR spectra of samples taken after 1, 4, 6 and 24 h of hydrothermal treatment are displayed in Fig. 2. It reveals that the product after 1 h hydrothermal crystallization would not show characteristic zeolite W adsorption bands, implying the sample obtained is amorphous aluminosilicate (Fig. 2a). The products crystallized from 4 to 24 h clearly display zeolite W characteristic bands. The adsorption bands at 768–442 cm^{-1} are related to the mixed vibration and deformation of silicon aluminum lattice. Furthermore, strong absorption band at about 1016 cm^{-1} for the valence vibration of (Al, Si)-O bonds. Also, the band relate to OH appear at about 1656 cm^{-1} (Fig. 2b–d) [17]. These results are in accord with the XRD results.

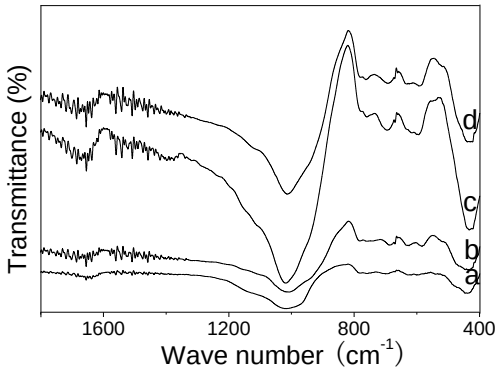

Fig. 2. FT-IR spectra of products with various crystallization time: (a) 1 h, (b) 4 h, (c) 6 h , (d) 24 h.

The SEM pictures of products obtained from various crystallization times are shown in Fig. 3. It is clearly observed that 1 h crystallized product consist of aggregated amorphous gel particles (Fig. 3a). It was reported that the existence of nuclei wrapped by amorphous mass, which could be verified by synchrotron in situ XRD [18]. A large number of amorphous particles are still present and the zeolite crystals are embedded in the amorphous entities after 3 h of hydrothermal treatment, which are reflected by XRD patterns with weak peaks (Fig. 3b). A small number of amorphous particles co-exist with loosely packed zeolite crystals are found after 4 h (Fig. 3c). After 5 h crystallization, the synthesized zeolite W crystals show twin-ball shaped morphology, the traces of amorphous material could also be observed (Fig. 3d). With the crystallization time further increase to 6 and 24 h, well-developed twin-ball shaped crystals are the main fraction of the samples, with ball diameter range of 12–16 μm (Fig. 3e–f). The above results are all in accord with the XRD and IR results. Moreover, the long crystallization time would not result in substantial changes in crystal morphology and size of end products.

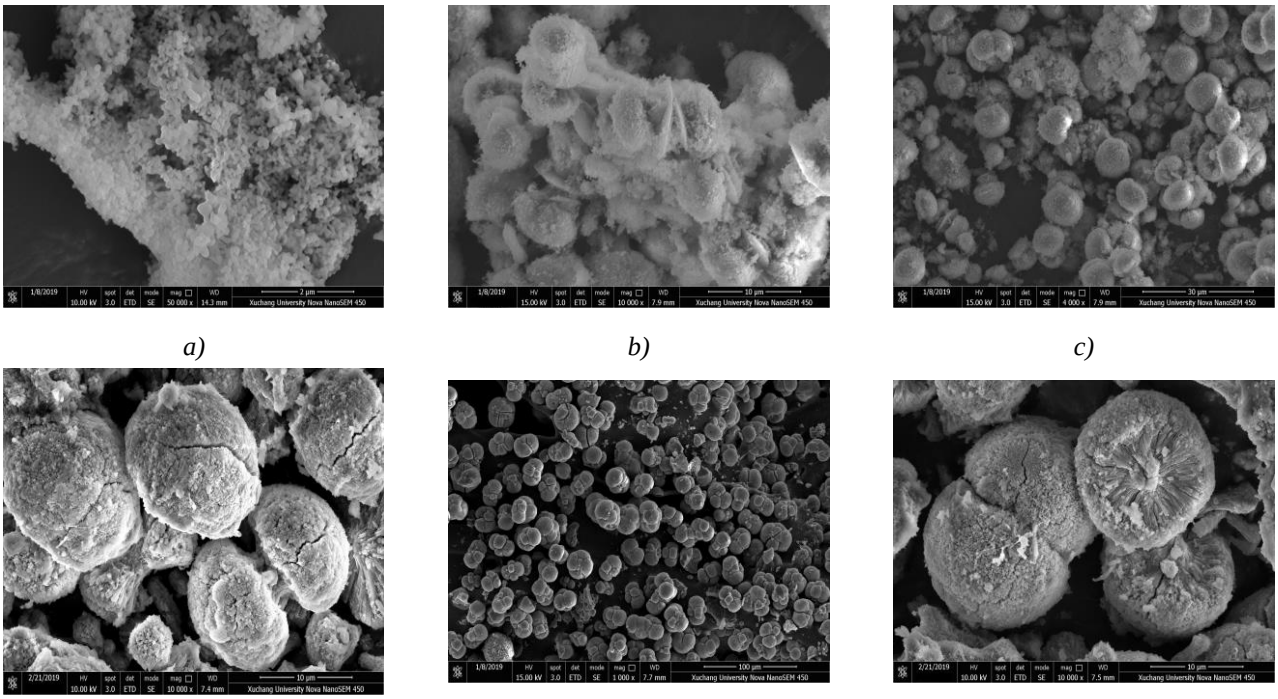

a) *b)* *c)*

d) *e)* *f)*

Fig. 3. SEM pictures of products obtained with various crystallization time. (a) 1 h, (b) 3 h, (c) 4 h, (d) 5 h, (e) 6 h and (f) 24 h.

3.2. Influence of aging time

Fig. 4 displays the influence of aging time on final products from the gel with mole ratio 1.5 K_2O: 0.1 Al_2O_3: 1.0 SiO_2: 57 H_2O, the gel was then hydrothermally crystallized at 150 °C for 6 h after 0–24 h aging under room temperature. For all samples, well-crystallized zeolite W crystals are formed. Therefore, the aging time would not have a significant influence on the crystallinity of zeolite W sample, this can be explained that the long crystallization time and high crystallization temperature which make the influence of aging time on the crystallinity negligible.

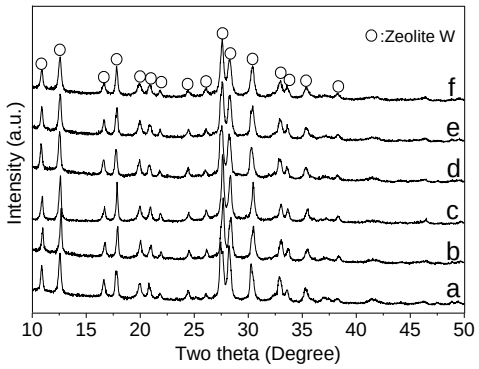

Fig. 4. XRD patterns of products obtained from various aging time. (a) 0 h, (b) 1 h, (c) 3 h, (d) 6 h, (e) 12 h, and (f) 24 h.

The corresponding SEM pictures are shown in Fig. 5. As shown in Fig. 5a, almost all of the products obtained without any aging process remain twin-ball shaped morphology. Bouquet-like shaped morphology of zeolite W crystals can be seen in addition to twin-ball crystals with aging time vary form 1 to 6 h (Fig. 5b–d). Also, it can be seen that the number of bouquet-like zeolite W crystals increase with the prolongation of aging time. When the aging time is increased to 12 and 24 h, zeolite W samples obtained are mostly bouquet-like in shape (Fig. 5e–f). Clearly, the aging step prior to crystallization strongly affects the crystal morphology and size of end products by the increase in the number nuclei, an increase in aging time favors the formation of smaller bouquet-like shaped zeolite W crystals. Caballero et al. [19] have reported that too short aging time would result in the occurrence of undesired nucleation of the competing phase, which hampered the crystallization crystallinity in the zeolite samples. However, in our case, no amorphous material or peak of other phase is seen in the final products with short aging time.

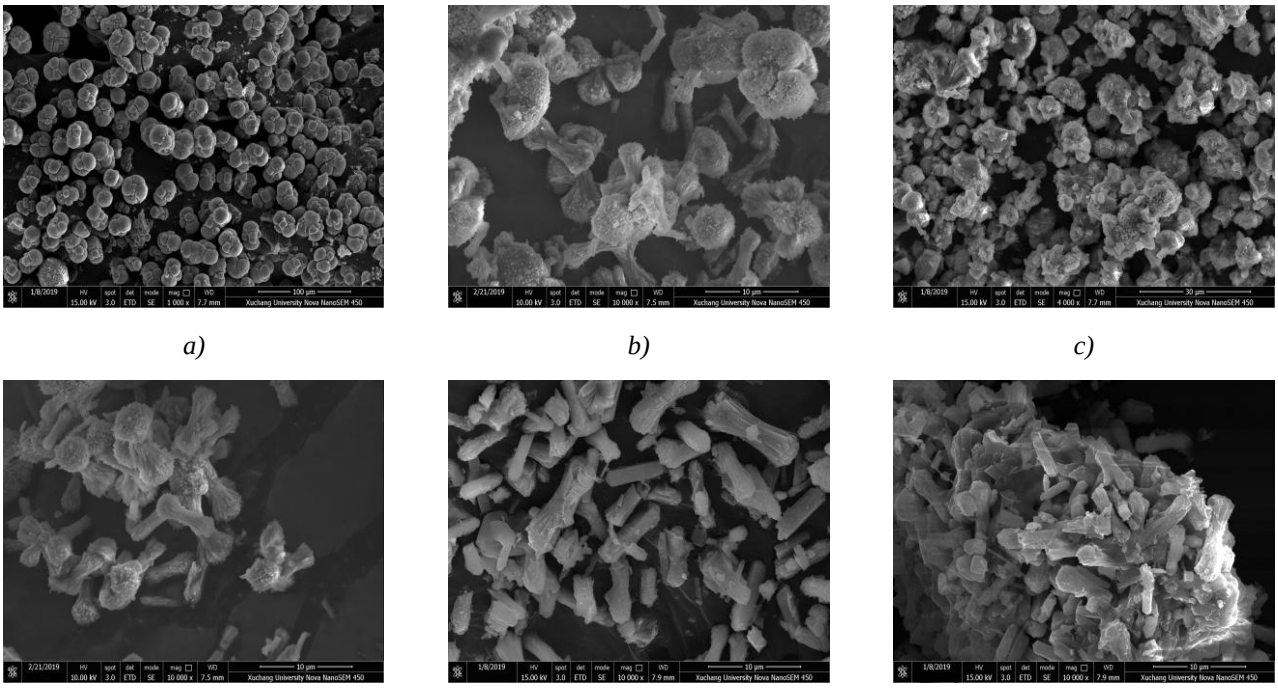

a) *b)* *c)*

d) *e)* *f)*

Fig. 5. SEM pictures of products obtained from various aging time. (a) 0 h, (b) 1 h, (c) 3 h, (d) 6 h, (e) 12 h, and (f) 24 h.

3.3. Influence of aging temperature

Fig. 6 displays the influence of aging temperature on final products from the gel with mole ratio 1.5 K_2O: 0.1 Al_2O_3: 1.0 SiO_2: 57 H_2O, the gel was then hydrothermally crystallized at 150 °C for 6 h after 1 h aging under 25 (room temperature), 70, 120 and 180 °C, respectively. Fig. 6 clearly reveals that well-crystallized zeolite W could be obtained with aging temperature is increased from 25 to 120 °C (Fig. 6a–c). However, with aging temperature is increased to 180 °C, a small number of zeolite F is coexistent (Fig. 6d). These results confirm that the aging temperature plays a significant role in the nucleation process. The structure rearrangement happens at the aging stage and causes zeolite nuclei formation in the gel, an appropriate aging temperature could contribute to the formation of a well-tuned precursor, while the inappropriate aging temperature results in the occurrence of undesired nucleation [20,21]. Herein, the mother liquor is allowed to age at a low temperature and then crystallized at an elevated temperature. This report was supported by Caballero et al [19], who pointed that pure NaX crystals were formed only with aging temperature of 20–60 °C. Also, De Lucas et al. [22] reported that high aging temperature would result in the appearance of zeolite NaP in the zeolite NaA synthesis, meanwhile, the increase of aging temperature would lead to larger zeolite particle.

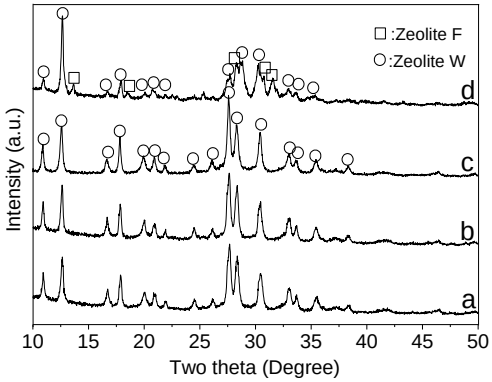

Fig. 6. XRD patterns of products obtained from various aging temperature. (a) 25 °C, (b) 70 °C, (c) 120 °C, and (d) 180 °C.

3.4. Influence of Al_2O_3/SiO_2

The XRD patterns of products obtained from various Al_2O_3 from 1.5 K_2O: x Al_2O_3: 1.0 SiO_2: 57 H_2O are shown in Fig. 7, the gel was then hydrothermally crystallized at 150 °C for 6 h after 1 h aging under room temperature. It can be seen that the product obtained at Al_2O_3/SiO_2=0.04 is poorly crystallized zeolite W (Fig. 7a). A gradual increase in the crystallinity is observed with the Al_2O_3/SiO_2 molar ratio is increased to 0.10 (Fig. 7b–c). The intensity of the peaks changes little with Al_2O_3/SiO_2=0.20 (Fig. 7d). However, with Al_2O_3/SiO_2 molar ratio is sequentially increased to 0.28, the characteristic peaks for zeolite W suddenly weaken and those identified as zeolite F develop (Fig. 7e). When Al_2O_3/SiO_2=0.45, the peaks of zeolite W completely disappear and the diffraction intensity of zeolite F increased, implying pure phase zeolite F is produced (Fig. 7f).

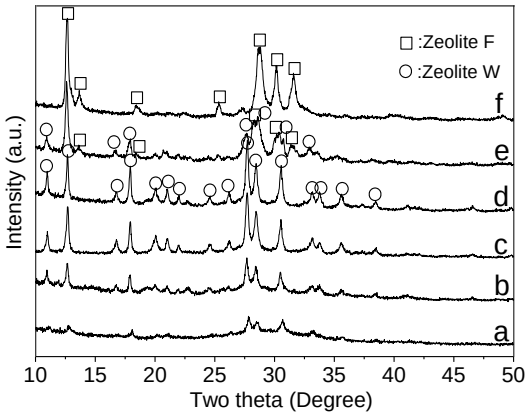

Fig. 7. XRD patterns of products obtained from the gel with various Al_2O_3/SiO_2 ratio. x: (a) 0.04, (b) 0.06, (c) 0.10, (d) 0.20, (e) 0.28, and (f) 0.45.

The SEM pictures of products obtained from Al_2O_3/SiO_2 molar ratio of 0.04, 0.20, 0.28 and 0.45 are shown in Fig. 8. As can been seen, with Al_2O_3/SiO_2=0.04, loosely packed zeolite crystals accompany with a large number of amorphous particles are observed (Fig. 8a–b). Well-developed twin-ball shaped morphology and some bouquet-like shaped morphology of zeolite W crystals are obtained with Al_2O_3/SiO_2=0.20 (Fig. 8c), and the SEM pictures taken at higher magnification reveal zeolite W crystals are composed of many square pillars crystals, with average width in the range of 0.2–0.5 μm and length approximately 10 μm (Fig. 8d). When Al_2O_3/SiO_2=0.28, flattened cuboid shape crystals due to zeolite F is seen in addition to twin-ball shape zeolite W crystals (Fig. 8e). The products generated at Al_2O_3/SiO_2=0.45 show only flattened cuboid shaped zeolite F crystals (Fig. 8f). The above results are all in accord with the XRD results. These results confirm that high Al_2O_3/SiO_2 molar ratio leads to the formation of zeolite F. This can be explained that the Al_2O_3/SiO_2 molar ratio increases with increasing sodium aluminate in the gel, the correspondingly higher Al^{3+} concentration favors small silicate species such as double four member ring (D4R) formation [23]. Similar results were the same as reported by Zhang [16] and Tanaka et al [24].

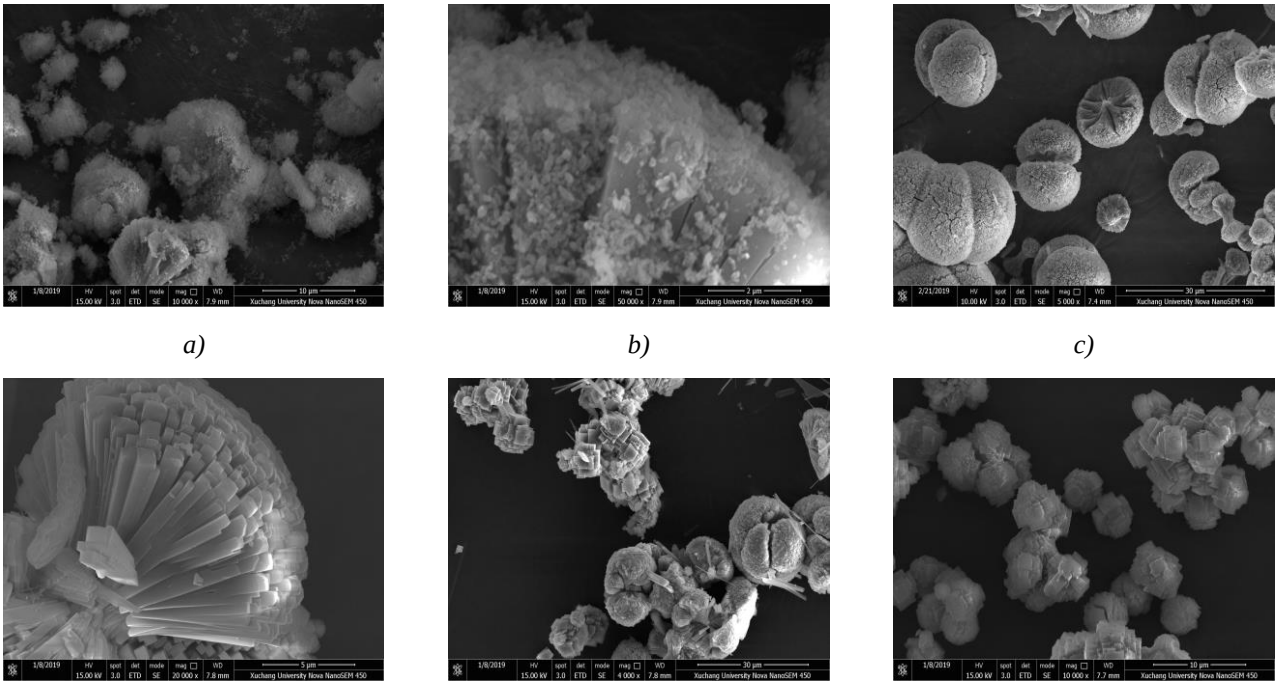

a) *b)* *c)*

d) *e)* *f)*

Fig. 8. SEM pictures of products obtained from the gel with various Al_2O_3/SiO_2 ratio. x: (a and b) 0.04, (c and d) 0.20, (e) 0.28: zeolite W + zeolite F, (f) 0.45: zeolite F.

3.5. Influence of K_2O/SiO_2

The XRD patterns of products obtained from various K_2O from y K_2O: 0.1 Al_2O_3: 1.0 SiO_2: 57 H_2O are shown in Fig. 9, the gel was then hydrothermally crystallized at 150 °C for 6 h after 1 h aging under room temperature. As a result, the product obtained with K_2O/SiO_2=0.15 is totally amorphous (Fig. 9a). Poorly crystallized zeolite W could be obtained with K_2O/SiO_2=0.36 (Fig. 9b). Well-crystallized zeolite W samples are formed at relatively higher K_2O/SiO_2 molar ratios of 0.65, 3.0 and 5.14 (Fig. 9c–e). However, with the K_2O/SiO_2 is increased to 9.42, the product obtained is pure phase of zeolite LTJ (Fig. 9f).

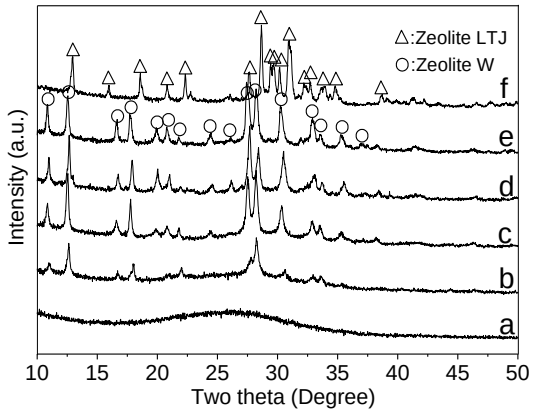

Fig. 9. XRD patterns of products obtained from the gel with various K_2O/SiO_2 ratio. y: (a) 0.15, (b) 0.36, (c) 0.65, (d) 3.0, (e) 5.14, and (f) 9.42.

The SEM pictures of products obtained from K_2O/SiO_2 molar ratio of 0.36, 0.65, 5.14 and 9.42 are shown in Fig. 10. Loosely packed zeolites W are embedded in aggregated amorphous materials are observed with K_2O/SiO_2=0.36 (Fig. 10a). Well-developed twin-ball shaped morphology and a small number of bouquet-like shaped morphology of zeolite W particles are obtained with K_2O/SiO_2 molar ratios 0.65 and 5.14 (Fig. 10b–c). It is clear that lower alkalinity in precursor solution is disadvantageous for the well-crystallized zeolite W produced. For Na_2O–Al_2O_3–SiO_2–H_2O system, the bigger the K_2O/SiO_2 molar ratio, the higher OH^- and the higher alkalinity will be. Generally speaking, high alkalinity results in good solubility of the Al and Si sources, and speeds up the polymerization of the aluminate and polysilicate anions [25]. Therefore, increase of alkalinity shortens the induction and nucleation periods. However, further increasing Na_2O/SiO_2 ratio more, too strong alkalinity promotes the autolysis of the samples obtained incipiently and leads to the decrease of relative crystallinity of produces, even impurity phase is formed. Duan et al. [26] have reported that zeolite L crystal was formed in low alkalinity circumstance, pure phase of zeolite W was obtained with increasing of the alkalinity, while the excessive high alkalinity led to the disappearance of zeolite W and made a transformation to form Natrolite. However, as shown in our case, no zeolite L is detected in low alkalinity circumstance. In case of K_2O/SiO_2=9.42, the irregular particle aggregates identified as zeolite LTJ are formed (Fig. 10d).

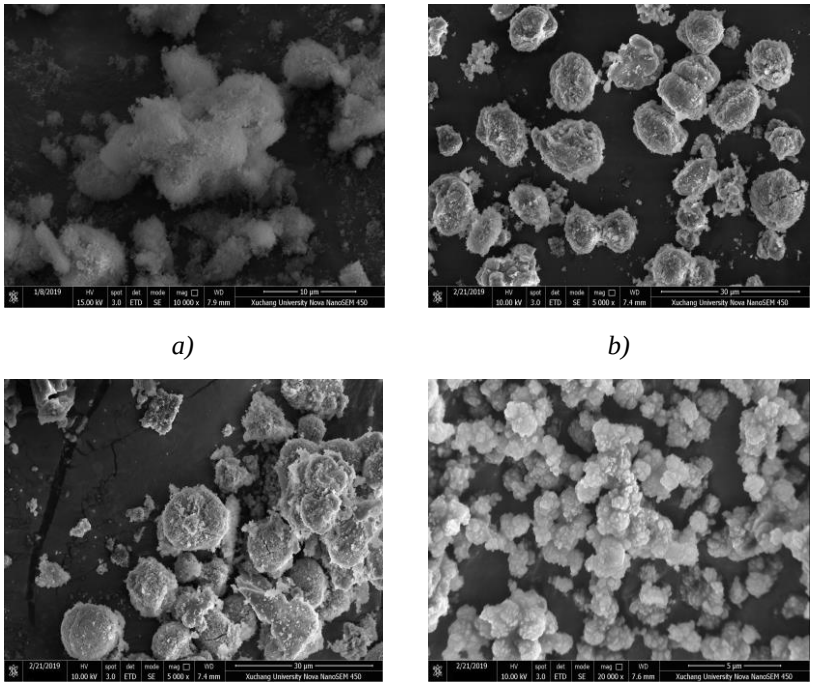

a) *b)*

c) *d)*

Fig. 10. SEM pictures of products obtained from the gel with various K_2O/SiO_2 ratio. y: (a) 0.36, (b) 0.65, (c) 5.14 and (d) 9.42: zeolite LTJ.

4. Conclusions

Well-developed twin-ball shaped morphology of zeolite W particles were obtained after 6 h of crystallization, further increasing crystallization time would not result in substantial change in

crystal morphology and size of final products. However, the crystals transferred from twin-ball to bouquet-like in shape with increasing aging time, with the aging time was increased to 12 and 24 h, the products obtained were mostly bouquet-like in shape. While the high aging temperature (T=180 °C) resulted in zeolite F developed. Moreover, the Al_2O_3/SiO_2 and K_2O/SiO_2 molar ratios of the gel had major influences on synthesis of pure form zeolite W.

A gradual increase in the crystallinity was observed with increasing Al_2O_3/SiO_2 molar ratio, however, too high Al_2O_3/SiO_2 (Al_2O_3/SiO_2=0.45) would lead to the formation of pure phase zeolite F. Also, mild alkalinity circumstance was in favor of zeolite W crystallization. When the K_2O/SiO_2 molar ratio was increased to 9.42, the product obtained was pure phase of zeolite LTJ.

Acknowledgments

Financial supports by the College Natural Science Foundation of Henan Province (17B530004).

References

[1] R. M. Barrer, Zeolites and Clay Minerals as Sorbents and Molecular Sieves, Academic Press, London, 1978.
[2] A. Dyer, An Introduction to Zeolite Molecular Sieve, John Wiley, London, 1988.
[3] A. M. Manta, D. L. Cursaru, S. Mihai, Dig. J. Nanomater. Bios. **14**, 509 (2019).
[4] J. Wen, H. Dong, G. Zeng, J. Clean. Prod. **197**, 1435 (2018).
[5] S. Yamaguchi, Y. Miyake, K. Takiguchi, D. Ihara, H. Yahiro, Catal. Today **303**, 249 (2018).
[6] M. Houlleberghs, E. Breynaert, K. Asselman, E. Vaneeckhaute, S. Radhakrishnan, M. W. Anderson, F. Taulelle, M. Haouas, J. A. Martens, C. E. A. Kirschhock, Micropor. Mesopor. Mat. **274**, 379 (2019).
[7] A. Medina, P. Gamero, J. M. Almanza, A. Vargas, A. Montoya, G. Vargas, M. Izquierdo, J. Hazard. Mater. **181**, 91 (2010).
[8] Y. H. Seo, E. A. Prasetyanto, N. Jiang, S. M. Oh, S. E. Park, Micropor. Mesopor. Mat. **128**, 108 (2010).
[9] X. Zhang, S. Li, G. Zhang, Dig. J. Nanomater. Bios. **14**, 705 (2019).
[10] T. Fukasawa, A. Horigome, A.D. Karisma, N. Maeda, A.N. Huang, K. Fukui, Adv. Powder Technol. **29**, 450 (2018).
[11] D. Matei, D. L. Cursaru, D. Stanica Ezeanu, Dig. J. Nanomater. Bios. **14**, 381 (2019).
[12] V. P. Valtchev, K. N. Bozhilov, M. Smaihi, L. Tosheva, Stud. Surf. Sci. Catal. **158**, 73 (2005).
[13] V. Valtchev, S. Rigolet, K. N. Bozhilov, Micropor. Mesopor. Mat. **101**, 73 (2007).
[14] A. K. Jamil, O. Muraza, A. M. Al-Amer, China Part. **24**, 138 (2016).
[15] J. Zhang, M. Li, Y. Lin, C. Liu, X. Liu, L. Bai, D. Hu, G. Zeng, Y. Zhang, W. Wei, Y. Sun, Micropor. Mesopor. Mat. **219**, 103 (2016).
[16] X. Zhang, D. Tang, M. Zhang, R. Yang, Powder Technol. **235**, 322 (2013).
[17] J. Hou, J. Yuan, R. Shang, Powder Technol. **226**, 222 (2012).
[18] V. P. Valtchev, K. N. Bozhilov, J. Phys. Chem. B **108**, 15587 (2004).
[19] I. Caballero, F. G. Colina, J. Costa, Ind. Eng. Chem. Res. **46**, 1029 (2007).
[20] D. Reinoso, M. Adrover, M. Pedernera, Ultrason. Sonochem. **42**, 303 (2018).
[21] B. Said, T. Cacciaguerra, F. Tancret, F. Fajula, A. Galarneau, Micropor. Mesopor. Mat. **227**,

176 (2016).
[22] A. De Lucas, M. A. Uguina, I. Covian, L. Rodriguez, Ind. Eng. Chem. Res. **32**, 1645 (1993).
[23] S. D. Kinrade, T. W. Swaddle, Inorg. Chem. **27**, 4253 (1988).
[24] H. Tanaka, Y. Sakai, R. Hino, Mater. Res. Bull. **37**, 1873 (2002).
[25] J. Zhu, Z. Liu, S. Sukenaga, M. Ando, H. Shibata, T. Okubo, T. Wakihara, Micropor. Mesopor. Mat. **268**, 1 (2018).
[26] A. Duan, T. Li, H. Niu, X. Yang, Z. Wang, Z. Zhao, G. Jiang, J. Liu, Y. Wei, H. Pan, Catal. Today **245**, 163 (2015).